THE JOURNAL OF PHYSICAL CHEMISTRY C

Article

pubs.acs.org/JPCC

Solvent Influence on the Role of Thiols in Growth of Thiols-Capped Au Nanocrystals

Yong Jiang,[†,¶,∥] Yuanyuan Huang,[†,∥] Hao Cheng,[†] Qinghua Liu,[†] Zhi Xie,[†] Tao Yao,*[,†] Zheng Jiang,[‡] Yuying Huang,[‡] Qing Bian,[§] Guoqiang Pan,[†] Zhihu Sun,*[,†] and Shiqiang Wei[†]

[†]National Synchrotron Radiation Laboratory, University of Science and Technology of China, Hefei, Anhui 230029, P.R. China

[‡]Shanghai Synchrotron Radiation Facility, Shanghai Institute of Applied Physics, Chinese Academy of Sciences, Shanghai 201204, P.R. China

[§]School of Science, PLA University of Science and Technology, Nanjing 211101, China

[¶]Hefei Center for Physical Science and Technology, Chinese Academy of Science, Anhui 230031, P.R. China

ABSTRACT: Solvent has a key role in the controllable synthesis of nanocrystals (NCs). Here, using X-ray absorption spectroscopy, we demonstrate that solvent can significantly influence the adsorption of thiols on Au NCs, and thereby affects their growth. It is shown that increasing the solvent polarities leads to the higher thiol coverage on the NC surface. The high coverage of thiols then retards the growth of particles, and as a result, the NCs' sizes decrease with the increase in the solvents' polarities. The underlying reason for the solvent dependence is proposed to be the synergistic effects of different hydrogen bond and hydrophobic interactions between the sulfhydryl and alkyl groups of thiols with the solvents molecules. This work addresses the important role of the solvent environments in the size-controlled synthesis of NCs.

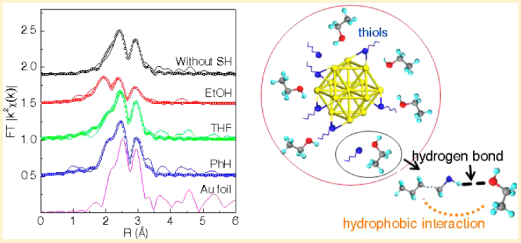

INTRODUCTION

Monodisperse spherical metal nanocrystals (NCs) with controlled size have fascinating size-dependent optical, electronic, catalytic, and chemical properties that make them highly important in applications in optics, electronics, and catalysis.[1−4] Particularly, monodisperse Au NCs of size in the range 1−5 nm are very interesting because they represent a bridge between bulk and molecular behavior.[5−9] For many years, remarkable advances have been made in the controllable synthesis of Au NCs.[10−12] However, to date, it is still a great challenge to rationally design the synthetic strategy to grow Au NCs with high monodispersity and controllable sizes. The main reason is that the underlying intrinsic roles of the reaction parameters, such as metal precursor, reductant, surfactant, and solvent, in controlling the processes toward NC formation are still poorly understood.

Mechanic studies have revealed that the manipulation of the growth processes is an effective means to achieve the controllable synthesis of NCs.[13−15] Because of the strong growth dependence on the surface status in the preparations of nanostructured matter, surfactants such as thiols become a practical way in controlling synthesis by modifying the surface of the Au NCs.[16,17] For example, in the Brust protocol, the size can be controlled mainly by adjusting the surfactant-to-precursor ratio; however, this is insufficient to synthesize monodisperse ultrasmall Au nanoparticles (<1.5 nm).[18] Recently, it has been found that the solvent can also be used to modulate the size, morphology, and the structures of the NCs. This is because the solvent provides an environment for the synthesis of NCs, which may have a large effect on the role of thiols in the particle growth process. For example, Song et al. found that the concentration of nuclei can be controlled by the fraction of solvent $CHCl_3$, which determined the final size of Au NCs.[19] Hyeon and co-workers found that the particle size of the iron oxide nanocrystals could be controlled by using solvents with different boiling points.[20] Nie et al. reported that conversion of hydrophilic gold nanorods into amphiphiles by selective replacement of surface ligands resulted in two-dimensional solvent-dependent organization of the nanorods.[21] Although these findings highlight the importance of solvent in the synthesis of nanomaterials, the critical role of solvents in the formation processes is rarely addressed.

In this work, we systematically investigate the solvent effect on the growth processes of Au NCs by varying the solvents polarities, using in situ X-ray absorption fine structure (XAFS) technique as a sensitive local-structural probe to determine the evolutions of atomic and electronic structures of the Au NCs. Three solvents with different polarities are chosen: ethanol (EtOH: C_2H_5OH) > tetrahydrofuran (THF: C_4H_8O) > benzene (PhH: C_6H_6). We find that the solvents exert strong impacts on the role of thiols during NCs growth, as reflected by the different coverage of the thiols and the Au−thiols interactions in the solvents with different polarities. A higher coverage of thiols is observed in the solvent with larger polarity,

Received: September 5, 2013
Revised: December 16, 2013
Published: December 17, 2013

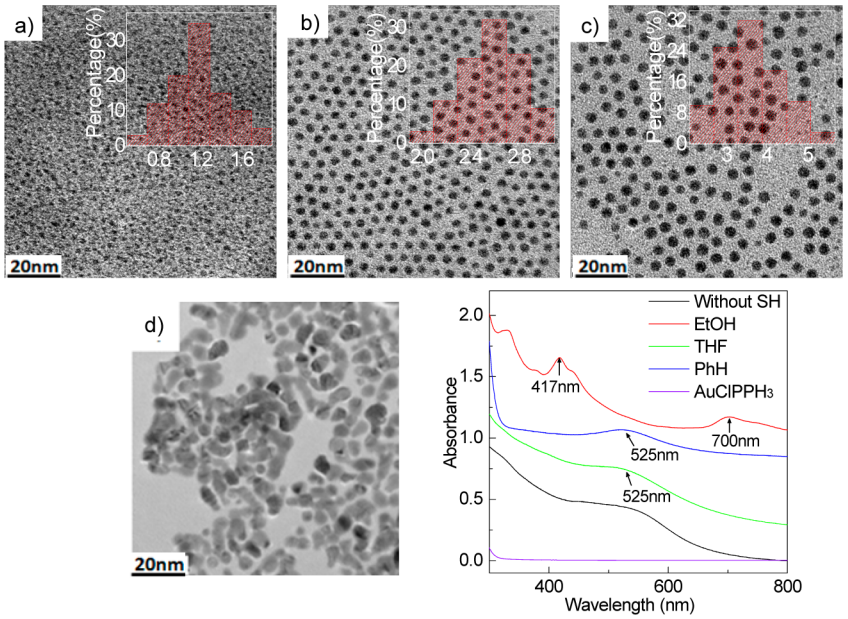

Figure 1. TEM images for the Au NCs synthesized via the reduction of $AuPPh_3Cl$ with TBAB for 8 h in (a) EtOH, (b) THF, (c) PhH in the presence of dodecanethiol, and (d) EtOH in the absence of dodecanethiol. The insets show the corresponding size distributions. (e) UV−vis spectra of Au NCs synthesized in different solvents in the presence of dodecanethiol. The spectra for Au NCs prepared in EtOH without dodecanethiol, and the precursor $AuClPPh_3$, are shown for comparison.

and consequently, this effect inhibits the growth of the particles, leading to a smaller size of Au NCs.

EXPERIMENTAL SECTION

Materials. Tetrachloroauric acid (Aldrich, 99.9+%), dodecanethiol (Aldrich, $C_{12}H_{26}S$,), ethanol, tetrahydrofuran, benzene, triphenylphosphine (Aldrich, PPh_3), and *tert*-butylamine-borane (Aldrich, TBAB) were used as received without further purification. $ClAuPPh_3$, in the form of white powder, was synthesized by reacting $HAuCl_4{\cdot}nH_2O$ with PPh_3.

Preparation of Dodecanethiol-Capped Au NCs. The 0.016 g of $AuClPPh_3$ was dissolved in 5 mL solvents (C_2H_5OH, C_4H_8O, and C_6H_6) at room temperature. Then 8 μL of dodecanethiol was added to the solution. After 2 min, 0.027 g of TBAB was dissolved in the mixture. The mixture was stirred continuously for 10 h to form thiol-capped Au NCs.

Characterizations and Analyses. TEM images were obtained with a JEOL 2010 system. The samples for TEM were prepared by dropping the reaction solution onto Cu TEM grids directly and drying in air. The UV−vis spectra were recorded on a UV-2501PC/2550 spectrophotometer in the wavelength range of 200−800 nm, and corrected by ethanol as background absorption. As reference, the initial precursor solution was also measured. In situ XAFS measurements were performed in transmission mode at the U7C XAFS station in National Synchrotron Radiation Laboratory, China, 1W1B beamline of Beijing Synchrotron Radiation Facility, China, and BL14W1 beamline of Shanghai Synchrotron Radiation Facility, China, using ionization chambers with optimized detecting gases to measure the radiation intensity. The storage ring of SSRF worked at 3.5 GeV with a maximum current of 210 mA. Au NCs samples used in XAFS measurement are homogeneously dispersed in the solution phase to preserve their real status without precipitation. The liquid samples were taken out directly from the reaction vessels into a Teflon cell. Considering that the concentration of Au is about 6.4 mM, the in situ Teflon cell is designed to have a path length in X-ray direction of about 10 mm that results in the absorption jump of ~0.2, so as to obtain good signal-to-noise XAFS data. The Au foil was also measured for comparison. The quantitative information can be obtained by the least-squares curve fitting in the *R*-space with a Fourier transform *k*-space range of 2.2−12.5 $Å^{-1}$ (typical *R* ranges were 1.3−3.2 Å) in a Kaiser-Bessel window, using the module ARTEMIS of programs of IFEFFIT.[22] Effective scattering amplitudes and phase shifts for the Au−S and Au−Au pairs were calculated with the ab initio code FEFF8.0. The structural parameters, such as the coordination number CN, the interatomic distance *R*, the Debye−Waller factor σ^2, and the edge-energy shift ΔE_0, were allowed to vary during the fitting process.

RESULTS AND DISCUSSION

Figure 1a−c shows the TEM images of the Au NCs synthesized in the solvents with different polarities, and their corresponding size distributions are shown as well. We can find that all particles are in spherical shape and of high monodispersity with a narrower size distribution smaller than 0.4 nm. Furthermore, the size of the obtained NC gradually increases when the polarities of the solvents decrease. The average particle sizes in various solvents are found to be 1.2, 2.5, and 3.4 nm in EtOH, THF, and PhH, respectively. Because the only changed parameter in the synthesis of all Au NCs here is solvents with different polarities, the results clearly suggest that varying solvents can effectively achieve the size-controlled synthesis. For comparison, we also prepared Au NCs in the absence of thiols by reducing the $AuClPPh_3$ precursor with TBAB in EtOH (Figure 1d). It can be found that the obtained particles have a larger size with severe particles aggregation. This indicates that the presence of thiol ligand is crucial for the preparation of small, monodisperse Au NCs since thiol is an efficient etchant.[17,23] The UV−vis spectra also confirm the above size evolutions. For NCs obtained in PhH and THF with

dx.doi.org/10.1021/jp408926n | J. Phys. Chem. C 2014, 118, 714−719

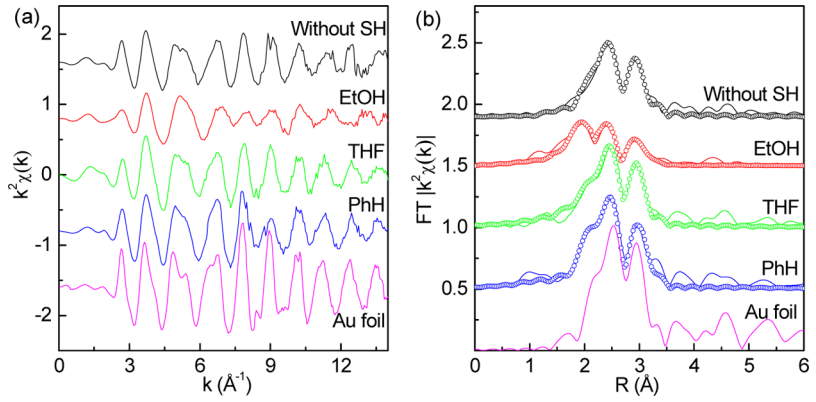

Figure 2. Au L_3-edge k^2-weighted extended X-ray absorption fine structure oscillations $[k^2\chi(k)]$ (a) and their Fourier transforms (b) for the samples and the foil. The samples are noted as their corresponding solvents. The empty circles in (b) show the fitting results.

Table I. Structural Parameters of Au NCs Extracted from Least-Squares Curve Fitting of the EXAFS FT Peaks by Separating the Contributions of Au Atoms at the Surface and in the Core of the Particles[a]

sample	bond	p^b	R (Å)	CN	σ^2 (10^{-3} Å)	ΔE
Au foil	Au−Au		2.88 ± 0.01	12	8.0 ± 0.3	3.5 ± 1.1
without SH	Au−Au		2.87 ± 0.02	10.5 ± 0.4	11.8 ± 0.6	4.5 ± 1.0
EtOH	Au−S		2.32 ± 0.03	1.7 ± 0.3	3.3 ± 0.3	3.2 ± 0.5
	Au−Au (surface)		2.81 ± 0.03	7.7 ± 0.5	12.0 ± 1.1	4.0 ± 1.1
	Au−Au (core)	0.24	2.88 ± 0.02	12	10.3 ± 1.0	4.1 ± 0.9
THF	Au−S		2.39 ± 0.03	1.2 ± 0.3	4.3 ± 0.3	3.2 ± 0.6
	Au−Au (surface)		2.84 ± 0.02	6.5 ± 0.3	10.2 ± 0.9	3.8 ± 1.1
	Au−Au (core)	0.63	2.88 ± 0.02	12	9.0 ± 0.9	4.4 ± 0.8
PhH	Au−S		2.42 ± 0.03	1.0 ± 0.2	3.8 ± 0.2	3.6 ± 0.6
	Au−Au (surface)		2.84 ± 0.02	6.1 ± 0.3	9.8 ± 0.9	3.8 ± 1.1
	Au−Au (core)	0.72	2.88 ± 0.02	12	9.0 ± 1.0	4.2 ± 0.8

[a]The Au−Au coordination numbers in the core of the NCs were fixed during the fitting. [b]p is the fraction of Au atoms in the core of the NCs.

thiols, as well as in the absence of thiols, the UV−vis spectra exhibit only intense surface plasmon band peaked at 510 nm that originated from the characteristic plasmon resonance absorbance for spherical Au NCs larger than 2 nm.[1] This absorbance intensifies and broadens with decreasing solvent polarity from THF to PhH, suggesting the increased NC size. However, for the NCs synthesized in EtOH, the spectral profile is highly structured and displays the fingerprint features of small Au nanoclusters with molecule-like electronic structure.[24] Given the key role of the surfactants in directing the NC growth, the solvent-dependent size evolution of Au NCs is largely due to the distinct effects of the solvents on the thiols that serve as the surfactant in the growth of Au NCs.

To investigate how the solvents influence the role of thiols, we plot in parts (a) and (b) of Figure 2 the EXAFS oscillation $k^2\chi(k)$ and the corresponding Fourier-transformed (FT) spectra for all NCs. The atomic structures of thiol-capped Au NCs synthesized in different solvents vary significantly, as reflected by the obviously different EXAFS oscillation shapes. Meanwhile, the NCs for the in situ measurement in solution are capped by dodecanethiol, which are different from those Au nanoclusters without capping agents measured in vacuum in a previous report.[25] Thus, the different samples states would consequently lead to the discrepancies in the shape and intensities in the EXAFS data. The corresponding FTs curves further identify the differences of Au−S and Au−Au bonding. For the thiol-capped Au NCs synthesized in EtOH, a strong Au−S coordination peak is observed at 1.85 Å, while for the NCs prepared in THF and PhH, the Au−S coordination peak is dampened and shifts toward high R position (1.89 Å), implying the strengthened Au−thiols interaction with increased solvent polarities. Taking into account the full reduction and the fact that dodecanethiol is a much stronger ligand than phosphine when binding to Au, we believe that these few and weak ligands can be replaced by dodecanethiol ligand within a very short time and have negligible influence on the following thiol ligand adsorption process. Therefore, we consider that the contribution of the coordination between Au and phosphine or chloride ligands should be small, and the FT peaks at around 1.85 Å are mainly from the Au−S pair. Moreover, the intensity of the Au−Au coordination peaked within 2.15−2.25 Å gradually decreases in the following order: in PhH > in THF > in EtOH. It should be noted that these variations are not directly related to the NC size, which can be inferred from the fact that the NCs synthesized without thiols have the lower Au−Au peak, although it has similar size to that prepared in PhH. We consider that the variations of the intensities of Au−Au peak mainly come from the structural disorder, as will be confirmed by the following fittings.

To obtain more insight into the Au−thiol interfacial interactions in different solvents, we further examine the solvent-dependent evolutions of the Au−S and Au−Au bonds. The contributions of Au atoms at the surface and in the core of a particle were separated in the fitting by defining a parameter p for the fraction of core atoms of the Au particle. The extracted structural parameters are listed in Table 1. Seen from Table 1, the Au−S bond has polarity-dependent lengths of 2.32, 2.39, and 2.42 (±0.03) Å and coordination numbers of 1.7, 1.2, and

dx.doi.org/10.1021/jp408926n | J. Phys. Chem. C 2014, 118, 714−719

1.0 (±0.3) from EtOH, THF, and PhH. For the synthesis conducted in EtOH, the NCs have a size of 1.2 nm, containing 25−38 Au atoms. In this case, the S atoms would occupy the surface bridge sites formed by two Au surface atoms and one head S atom as in a fully dodecanethiol-capped Au NC.[26,27] Hence, the dodecanethiol coverage can be conveniently calculated with the expression of $CN_{Au-S}/2.0$, while for the NCs prepared in THF and PhH, the dodecanethiol coverage can be calculated with the expression of $CN_{Au-S}/3.0$ since the S atoms would occupy the surface hollow sites with a typical tetrahedral configuration formed by three Au surface atoms and a head S atom.[28] Therefore, the dodecanethiol coverage were calculated as 0.85, 0.4, and 0.3 for the Au NCs prepared in EtOH, THF, and PhH, respectively. Of note, the mole ratio of alkanethiol to Au is near 1:1 in this work, smaller than that found in previous reports in which the *n*-alkanethiols are always in excess.[29,30] Hence, the coverage of 0.85 for NCs synthesized in EtOH is relatively smaller than that in previous cases of full capping. The evolutions of the coverage indicate that the solvents significantly affect the adsorption ability for the thiols on the NCs surface, and the thiols have a higher coverage in the solvents with larger polarities. During the synthesis and in situ measurement in this work, some amount of Cl or PPh_3 ligands are presented in the solution. However, due to the strong dependence of nanocrystals' states on their solvent environments, the surface status of the nanocrystals with low thiols coverage are inevitably changed and deviated from their natural states if they are isolated from THF and PhH solvents. Moreover, the main goal of this work is to investigate the real influence of the solvents on the thiols-capped nanocrystals. Hence, it is necessary to perform in situ measurement in which the nanocrystals are kept in their original solvent environment without post-treatments. Despite the existence of Cl or PPh_3 in the solution, they bound quite weakly on the as-formed nanocrystals, and hence contributing little to the FT peaks at 1.85 Å, which can be confirmed by our previous report.[31] Therefore, the determination of thiols coverage through the EXAFS fitting would be a more reliable method at current stage.

The difference in the coverage of thiols can also be reflected by the interactions between thiols and Au NCs. Figure 3 shows the Au L_3-edge XANES spectra, which are used to probe the Au−thiols interactions by estimating the charge transfer of Au and S. Upon comparison of Au NCs prepared in different solvents, we observe a noticeable increase of the white-line peak for the NCs prepared in the solvents with higher polarities,[32,33] corresponding to more *d*-charge transfer from Au atoms to S atoms. Upon comparison of Au NCs prepared in different solvents, we observe a noticeable increase of the white-line peak for the NCs prepared in the solvents with higher polarities. Following the method proposed in ref 32, we have calculated the total amounts of charge loss (5*d* hole counts (d_{hole} + $d_{electron}$ = 10)) for Au atoms, and obtained the values of ∼0.08, ∼0.04, and ∼0.03 e/atom for the nanocrystals in EtOH, THF, and PhH, respectively. The contribution from the size effects that induce the distinct *d*-charge loss can be adopted from the previous report in which the NCs capped by thiols are in a size range similar to those in this work.[32] Therefore, subtracting such contribution from the size effects, the contributions from the solvent effect can be estimated as ∼0.03, ∼0.004, and ∼0.002 e/atom, for the NCs in EtOH, THF, and PhH, respectively. This method at least reflects the trend that more *d*-charge transfers from Au atoms to S atoms when the NCs are prepared in strong polar solvents, implying that interactions between Au NCs and thiols are stronger for the NCs prepared in the solvents with larger polarities. Furthermore, the peaks B and C originating from multiple-scattering contributions in the post-E_0 gradually intensify with decreasing polarities, and the spectrum for the NCs obtained in PhH is close to that of Au foil. This implies that the structures of the NCs prepared in the solvent with weak polarities are more similar to that of Au foil, while the structure disorder of NCs is increased due to the enhanced Au−thiols interactions. Therefore, the enhanced white-line peak in the XANES spectra for the NCs synthesized in the solvents with higher polarities could be ascribed to the high coverage of thiols. Moreover, the fitting results show that the structural disorder for the surface Au atoms increases from 9.8 to 10.2 × 10^{-3} Å and then to 12.0 × 10^{-3} Å for the NCs prepared in the solvents with increased polarities, which are also probably due to the different coverage of thiols. Such increased surface disorder could lead to the dampened intensities of multiple-scattering peaks in XANES spectra and also of the Au−Au peaks in FTs.

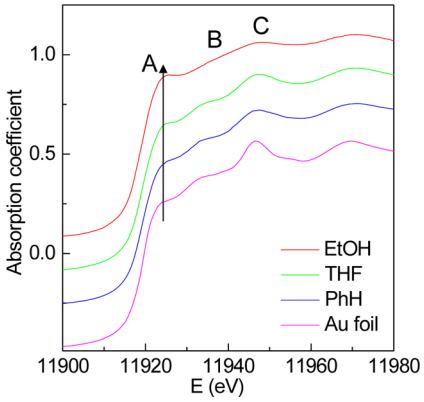

Figure 3. Au L_3-edge XANES data for Au NCs, along with the Au foil data for reference. Intensity for the white-line peak A increases with higher polarities as marked by the upward arrow.

The above results suggest that the coverage of thiols, as well as the strengths of the interaction between thiols and the NCs, decrease when decreasing the solvents' polarities. It is widely accepted that organic surfactants have a key role in determining not only the size but also the shape of the products.[16,34] Hence, the role of the thiols involved in the growth kinetics of Au NCs can be tuned through changing the solvents, and hence the pathways of the nucleation of monomers and the growth of nuclei can be controlled. In Figure 4, we schematically show the influence of the solvents on the thiols and the growth processes. We examine the interactions between the solvents and thiols to explain the difference in the coverage of thiols. For the ethanol with relatively strong polarity, the existence of the terminal hydroxyl group (−OH) has a favorable interaction with the thiols via hydrogen bond (noted by black frame in Figure 4).[35,36] And for THF, there is also a hydrogen bond interaction between oxygen in THF and H in the thiols, while the hydrogen bond would not be formed for the aprotic solvent of PhH with a symmetric benzene ring structure. For the first two cases, the electronegativity of O in EtOH is larger than that in THF, corresponding to a stronger hydrogen bond and more significant charge transfer from thiols to EtOH. Hence, we consider that there is more charge loss for the head group S atoms of thiols in EtOH, and the values of the charge density

dx.doi.org/10.1021/jp408926n | J. Phys. Chem. C 2014, 118, 714−719

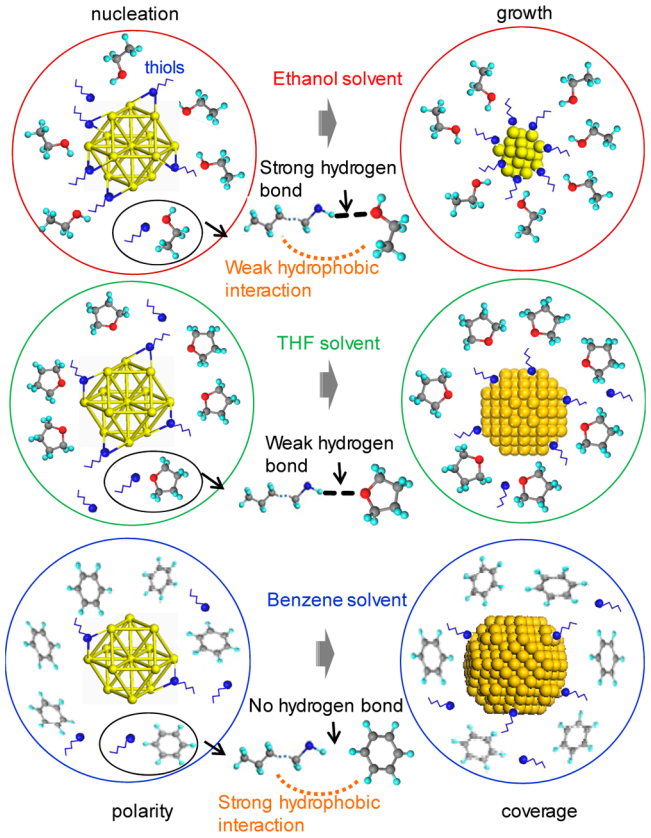

Figure 4. Schematic representation of the influences of three solvents on the growth processes in the chemical synthesis of Au NCs. Because of the difference in the strength of the hydrogen bond and hydrophobic interactions between the sulfhydryl groups of thiols with the solvent molecules, the thiols have different coverage on the NCs surface.

for the S atoms is in the following order: in EtOH < in THF < in PhH. Consequently, the less charge density of S atoms would facilitate the Au charge transfer from Au atoms to S atoms, and promotes the adsorption of thiols on Au clusters. However, because the alkyl groups in the dodecanethiol and the PhH are similar in their weak polarities and in their carbon chain,[37] a strong hydrophobic interaction exists between PhH and the alkyl group of dodecanethiol, which is weak for the dodecanethiol in polar solvent EtOH. The strong hydrophobic interaction between the solvent molecule and the thiols may inhibit the adsorption of the thiols on the surface of the clusters.

Therefore, we consider that the hydrogen bond and the hydrophobic effects would change the coverage of the dodecanethiol on the Au NCs. As determined by the above-fitted results, the coverage of the solvents is in the following order: in EtOH > in THF > in PhH. The effect of solvent molecule on the thiol-capped Au nuclei has also been inferred by Toikkanen et al. who found that the stability of hexanethiolate-protected Au_{38} clusters is critically dependent on the dispersing solvent.[38] As the polarities of solvents decrease, the size of the nuclei becomes smaller with larger particle density; that is, the size control is preliminary achieved by the solvent-controlled nucleation. For the later growth process, it has been reported that interparticle coalescence plays a critical role. For instance, by using in situ TEM technique, Zheng et al. observed that the platinum NCs grow in size by merging with another NC in random coalescence events and thereby jumping ahead in the growth race.[39] Also, in our previous in situ studies on the nucleation and growth of Au NCs by XAFS method, we have found the eventual coalescence in the later growth process.[15] As discussed above, the strong hydrogen bond interaction between the solvent molecule and thiols induces more absorption of thiols on the NC surface, and meanwhile, the hydrophobic effect between weak-polar solvents and the thiols leads to desorption of thiols on the NC surface. The high coverage of thiols would also permit the small Au clusters to adopt a slightly different geometry, which is supported by the general increase in the surface Au−Au bond lengths from 2.81 to 2.84 Å, and the decrease in the surface disorder for the NCs synthesized from EtOH to THF and then to PhH. Therefore, the high coverage effectively prevents the NCs coalescence and aggregation. The role of thiols in the NC growth stage can be reinforced by our comparative experiment: even if the NC is synthesized in EtOH solvent, the particle size is still large without the addition of thiols.

CONCLUSION

In summary, this work addresses the important influence of the solvent that is overlooked in the size-controlled synthesis of Au NCs, via modulating the role of the thiol ligands and their interactions with NCs. The analysis of in situ XAFS results indicates that there is higher coverage of thiols for the NCs synthesized in the solvents with larger polarities. This is primarily due to the synergistic effects of hydrogen bond interaction in the polar solvent and the hydrophobic interaction between the weak-polar solvents and alkyl group of dodecanethiol. Regarding this solvent effect, we would try the possibility of sulfur K-edge absorption study based on soft X-ray, which could give some more information to further prove this point. The high coverage of thiols results in smaller nuclei formed in the nucleation, and further screens the interparticle van der Waals attraction in the growth stage, leading to a smaller size of NCs.

AUTHOR INFORMATION

Corresponding Author

*T.Y.: e-mail, yaot@ustc.edu.cn; tel., +86-551-63601997. Z.H.S.: e-mail, zhsun@ustc.edu.cn; tel.: +86-551-63601992-1026.

Author Contributions

‖These authors contributed equally to this work.

Notes

The authors declare no competing financial interest.

ACKNOWLEDGMENTS

This work was supported by the National Natural Science Foundation of China (11135008, 11205158, U1232132, 11175184, 11079032, and 11075164), the National Basic Research Program of China (2012CB825800), by the Foundation for Innovative Research Groups of the National Natural Science Foundation of China (11321503), and by the Fundamental Research Funds for the Central Universities (WK2310000023, WK2310000024, and WK2310000026). The authors would like to thank NSRL, BSRF, and SSRF for the beam time.

REFERENCES

(1) Talapin, D. V.; Lee, J. S.; Kovalenko, M. V.; Shevchenko, E. V. Prospects of Colloidal Nanocrystals for Electronic and Optoelectronic Applications. *Chem. Rev.* **2009**, *110*, 389−458.

(2) Xia, Y.; Xiong, Y.; Lim, B.; Skrabalak, S. E. Shape-Controlled Synthesis of Metal Nanocrystals: Simple Chemistry Meets Complex Physics? *Angew. Chem., Int. Ed.* **2009**, *48*, 60−103.

(3) Park, J.; Joo, J.; Kwon, S. G.; Jang, Y.; Hyeon, T. Synthesis of Monodisperse Spherical Nanocrystals. *Angew. Chem., Int. Ed.* **2007**, *46*, 4630−4660.

(4) Lohse, S. E.; Murphy, C. J. Applications of Colloidal Inorganic Nanoparticles: From Medicine to Energy. *J. Am. Chem. Soc.* **2012**, *134*, 15607−15620.

(5) Daniel, M. C.; Astruc, D. Gold Nanoparticles: Assembly, Supramolecular Chemistry, Quantum-Size-Related Properties, and Applications Toward Biology, Catalysis, and Nanotechnology. *Chem. Rev.* **2004**, *104*, 293−346.

(6) Pyykko, P. Theoretical Chemistry of Gold. *Angew. Chem., Int. Ed.* **2004**, *43*, 4412−4456.

(7) Lopez-Sanchez, J. A.; Dimitratos, N.; Hammond, C.; Brett, G. L.; Kesavan, L.; White, S.; Miedziak, P.; Tiruvalam, R.; Jenkins, R. L.; Carley, A. F.; et al. Facile Removal of Stabilizer-Ligands from Supported Gold Nanoparticles. *Nat. Chem.* **2011**, *3*, 551−556.

(8) Turner, M.; Golovko, V. B.; Vaughan, O. P. H.; Abdulkin, P.; Berenguer-Murcia, A.; Tikhov, M. S.; Johnson, B. F. G.; Lambert, R. M. Selective Oxidation with Dioxygen by Gold Nanoparticle Catalysts Derived From 55-Atom Clusters. *Nature* **2008**, *454*, 981−983.

(9) Tedsree, K.; Chan, C. W. A.; Jones, S.; Cuan, Q. A.; Li, W. K.; Gong, X. Q.; Tsang, S. C. E. C-13 NMR Guides Rational Design of Nanocatalysts via Chemisorption Evaluation in Liquid Phase. *Science* **2011**, *332*, 224−228.

(10) Sun, Y. G.; Xia, Y. N. Shape-Controlled Synthesis of Gold and Silver Nanoparticles. *Science* **2002**, *298*, 2176−2179.

(11) Ji, X. H.; Song, X. N.; Li, J.; Bai, Y. B.; Yang, W. S.; Peng, X. G. Size Control of Gold Nanocrystals in Citrate Reduction: The Third Role of Citrate. *J. Am. Chem. Soc.* **2007**, *129*, 13939−13984.

(12) Zheng, N. F.; Fan, J.; Stucky, G. D. One-step One-Phase Synthesis of Monodisperse Noble-Metallic Nanoparticles and Their Colloidal Crystals. *J. Am. Chem. Soc.* **2006**, *128*, 6550−6551.

(13) Rempel, J. Y.; Bawendi, M. G.; Jensen, K. F. Insights into the Kinetics of Semiconductor Nanocrystal Nucleation and Growth. *J. Am. Chem. Soc.* **2009**, *131*, 4479−4489.

(14) Yao, T.; Liu, S. J.; Sun, Z. H.; Li, Y. Y.; He, S.; Cheng, H.; Xie, Y.; Liu, Q. H.; Jiang, Y.; Wu, Z. Y.; et al. Probing Nucleation Pathways for Morphological Manipulation of Platinum Nanocrystals. *J. Am. Chem. Soc.* **2012**, *134*, 9410−9416.

(15) Yao, T.; Sun, Z. H.; Li, Y. Y.; Pan, Z. Y.; Wei, H.; Xie, Y.; Nomura, M.; Niwa, Y.; Yan, W. S.; Wu, Z. Y.; et al. Insights Into Initial Kinetic Nucleation of Gold Nanocrystals. *J. Am. Chem. Soc.* **2010**, *132*, 7696−7701.

(16) Yin, Y.; Alivisatos, A. P. Colloidal Nanocrystal Synthesis and the Organic-Inorganic Interface. *Nature* **2005**, *437*, 664−670.

(17) Vericat, C.; Vela, M. E.; Benitez, G.; Carro, P.; Salvarezza, R. C. Self-Assembled Monolayers of Thiols and Dithiols on Gold: New Challenges for a Well-Known System. *Chem. Soc. Rev.* **2010**, *39*, 1805−1834.

(18) Brust, M.; Walker, M.; Bethell, D.; Schiffrin, D. J.; Whyman, R. Synthesis of Thiol-Derivatised Gold Nanoparticles in a Two-Phase Liquid-Liquid System. *J. Chem. Soc., Chem. Commun.* **1994**, 801−802.

(19) Song, J.; Kim, D.; Lee, D. Size Control in the Synthesis of 1−6 nm Gold Nanoparticles via Solvent-Controlled Nucleation. *Langmuir* **2011**, *27*, 13854−13860.

(20) Park, J.; An, K. J.; Hwang, Y. S.; Park, J. G.; Noh, H. J.; Kim, J. Y.; Park, J. H.; Hwang, N. M.; Hyeon, T. Ultra-Large-Scale Syntheses of Monodisperse Nanocrystals. *Nat. Mater.* **2004**, *3*, 891−895.

(21) Nie, Z. H.; Fava, D.; Kumacheva, E.; Zou, S.; Walker, G. C.; Rubinstein, M. Self-Assembly of Metal-Polymer Analogues of Amphiphilic Triblock Copolymers. *Nat. Mater.* **2007**, *6*, 609−614.

(22) Ravel, B.; Newville, M. ATHENA, ARTEMIS, HEPHAESTUS: Data Analysis for X-ray Absorption Spectroscopy Using IFEFFIT. *J. Synchrotron Rad.* **2005**, *12*, 537−541.

(23) Qian, H.; Zhu, Y.; Jin, R. C. Size-Focusing Synthesis, Optical and Electrochemical Properties of Monodisperse $Au_{38}(SC_2H_4Ph)_{24}$ Nanoclusters. *ACS Nano* **2009**, *3*, 3795−3803.

(24) Li, Y. Y.; Cheng, H.; Yao, T.; Sun, Z. H.; Yan, W. S.; Jiang, Y.; Xie, Y.; Sun, Y. F.; Huang, Y. Y.; Liu, S. J.; et al. Hexane-Driven Icosahedral to Cuboctahedral Structure Transformation of Gold Nanoclusters. *J. Am. Chem. Soc.* **2012**, *134*, 17997−18003.

(25) Balerna, A.; Bernieri, E.; Picozzi, P.; Reale, A.; Santucci, S.; Burattini, E.; Mobilio, S. A. Structural Investigation on Small Gold Clusters by EXAFS. *Surf. Sci.* **1985**, *156*, 206−213.

(26) Jadzinsky, P. D.; Calero, G.; Ackerson, C. J.; Bushnell, D. A.; Kornberg, R. D. Structure of a Thiol Monolayer-Protected Gold Nanoparticle at 1.1 Å Resolution. *Science* **2007**, *318*, 430−433.

(27) Tang, Z.; Xu, B.; Wu, B.; Germann, M. W.; Wang, G. Synthesis and Structural Determination of Multidentate 2,3-Dithiol-Stabilized Au Clusters. *J. Am. Chem. Soc.* **2010**, *132*, 3367−3374.

(28) Jiang, Y.; Yin, P. D.; Li, Y. Y.; Sun, Z. H.; Liu, Q. H.; Yao, T.; Cheng, H.; Hu, F. C.; Xie, Z.; He, B.; et al. Modifying the Atomic and Electronic Structures of Gold Nanocrystals via Changing the Chain Length of n-Alkanethiol Ligands. *J. Phys. Chem. C* **2012**, *116*, 24999−25003.

(29) Ackerson, C. J.; Jadzinsky, P. D.; Kornberg, R. D. Thiolate Ligands for Synthesis of Water-Soluble Gold Clusters. *J. Am. Chem. Soc.* **2005**, *127*, 6550−6551.

(30) Corthey, G.; Giovanetti, L. J.; Ramallo-López, J. M.; Zelaya, E.; Rubert, A. A.; Benitez, G. A.; Requejo, F. G.; Fonticelli, M. H.; Salvarezza, R. C. Synthesis and Characterization of Gold@Gold(I)-Thiomalate Core@Shell Nanoparticles. *ACS Nano* **2010**, *4*, 3413−3421.

(31) Cheng, H.; Yang, L. N.; Jiang, Y.; Huang, Y. Y.; Sun, Z. H.; Zhang, J.; Hu, T. D.; Pan, Z. Y.; Pan, G. Q.; Yao, T.; et al. Adsorption Kinetic Process of Thiol Ligands on Gold Nanocrystals. *Nanoscale* **2013**, *5*, 11795−11800.

(32) Simms, G. A.; Padmos, J. D.; Zhang, P. Structural and Electronic Properties of Protein/Thiolate-Protected Gold Nanocluster with "Staple" Motif: A XAS, L-DOS, and XPS Study. *J. Chem. Phys.* **2009**, *131*, 214703−214709.

(33) Zhang, P.; Sham, T. X-Ray Studies of the Structure and Electronic Behavior of Alkanethiolate-Capped Gold Nanoparticles: The Interplay of Size and Surface Effects. *Phys. Rev. Lett.* **2003**, *90*, 245502.

(34) Goesmann, H.; Feldmann, C. Nanoparticulate Functional Materials. *Angew. Chem., Int. Ed.* **2010**, *49*, 1362−1395.

(35) Rodriguez, P.; Kwon, Y.; Koper, M. T. M. The Promoting Effect of Adsorbed Carbon Monoxide on the Oxidation of Alcohols on a Gold Catalyst. *Nat. Chem.* **2012**, *4*, 177−182.

(36) Tereshchuk, P.; Da Silva, J. L. F. Ethanol and Water Adsorption on Close-Packed 3d, 4d, and 5d Transition-Metal Surfaces: A Density Functional Theory Investigation with van der Waals Correction. *J. Phys. Chem. C* **2012**, *116*, 24695−24705.

(37) Chandler, D. Interfaces and the Driving Force of Hydrophobic Assembly. *Nature* **2005**, *437*, 640−647.

(38) Toikkanen, O.; Carlsson, S.; Dass, A.; Ronnholm, G.; Kalkkinen, N.; Quinn, B. M. Solvent-Dependent Stability of Monolayer-Protected Au_{38} Clusters. *J. Phys. Chem. Lett.* **2010**, *1*, 32−37.

(39) Zheng, H.; Smith, R. K.; Jun, Y. W.; Kisielowski, C.; Dahmen, U.; Alivisatos, A. P. Observation of Single Colloidal Platinum Nanocrystal Growth Trajectories. *Science* **2009**, *324*, 1309−1312.